

Supporting Information For:

Transfer Hydrogenation of Carbon Dioxide and Bicarbonate from Glycerol Under Aqueous Conditions

Jacob Heltzel, Matthew Finn, Diana Ainembabazi, Kai Wang, Adelina Voutchkova-Kostal*

Chemistry Department, the George Washington University, 800 22nd St NW, Suite 4000, Washington, DC 20052 (USA)

*Corresponding author contact: avoutchkova@gwu.edu

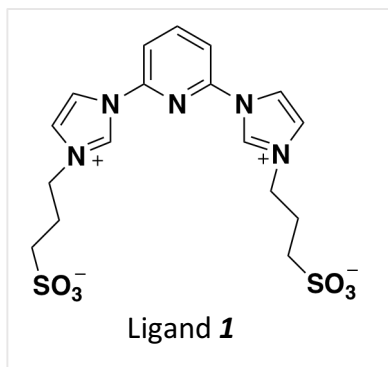
Table of Contents :

General Considerations	2
Synthesis of Catalyst <i>I</i>	2-3
Reaction Procedure	4
Product Characterization	4-5
Figure S1: Extract from HPLC chromatogram traces at 218 nm wavelength, showing authentic formic acid (FA), lactic acid (LA) and the t=4hr sample from Rxn A (6.85 M glycerol, catalyst <i>I</i> (5 mg), 150 °C, 26 bar CO ₂ , 2M KOH).	5
Table S1. Effect of temperature, pressure and KOH concentration on CO ₂ transfer hydrogenation reactions from glycerol with cat <i>I</i> .	6
Calculation of free energies of reaction (ΔG_{aq})	6
Figure S2. Time courses for production of formic acid (FA) and lactic acid (LA) from the reaction of CO ₂ and glycerol using 46 bar CO ₂ , 6.85 M glycerol, and 0.25 M KOH at (a) 150 °C and (b) 225 °C.	7
Figure S3. Time course for decomposition of formate in aqueous medium using catalyst <i>I</i> at 150 °C (0.15 mM cat <i>I</i> , 0.10 M formic acid, KOH(aq) to adjust pH, 50 mL total volume of water).	7
Figure S4. Additional visualization of the time course of reaction of K ₂ CO ₃ and glycerol using catalyst <i>I</i> (pN ₂ 26 Bar, 6.85 M aqueous glycerol, 2.00 M K ₂ CO ₃ , at 150 °C).	8
Figure S5. Section of ¹ H NMR spectra corresponding to t=0 (<i>1</i>), t=30 min (<i>2</i>), t=1h; t=90 min (<i>3</i>), for reaction of formic acid and glycerol to afford formate ester.	9
Table S2. Calculated free energies of reaction ($\Delta G^{\circ}_{\text{aq}}$) for the CO ₂ direct hydrogenation and transfer hydrogenation (Gaussian16, G3B3, PCM water).	10
References	11

General Considerations

Commercially available reagents were used without purification unless otherwise noted. $[\text{Ru}(p\text{-cymene})\text{Cl}_2]_2$ was purchased from Acros Organics. Anhydrous solvents were dried using a solvent purification system (SPS MBraun) or 4Å molecular sieves. Glycerol (>99%, Alfa Aesar) was dried over activated 4Å molecular sieves. NMR spectra were recorded on an Agilent NMR spectrometer operating at 400 MHz. HPLC analysis was carried out using a Shimadzu Prominence-i (LC-2030C 3D) instrument equipped with a PDA detector. Catalyst synthesis was performed using standard air-free Schlenk techniques.

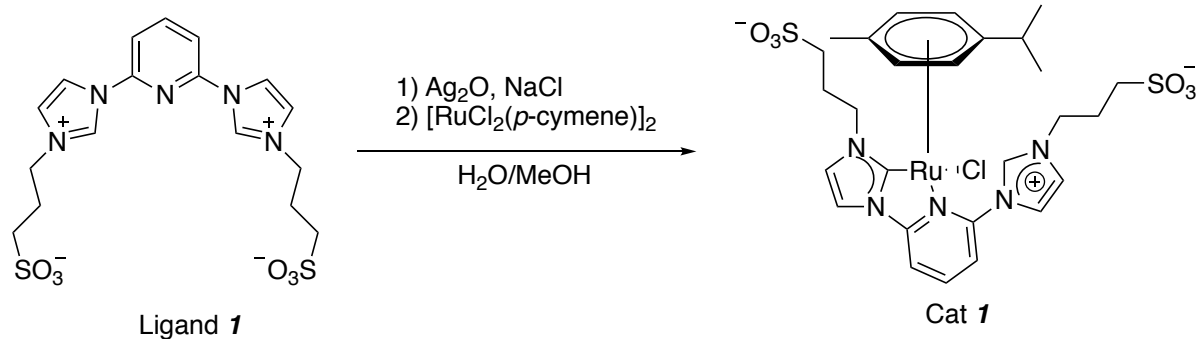
Synthesis of Catalyst 1



Ligand 1. Following a literature procedure,¹ 2,6-bis(1-imidazolyl)pyridine (0.538 g, 2.55 mmol) and 1,3-propane sultone (1.565 g, 12.8 mmol) were loaded in a high pressure Pyrex tube. Acetonitrile (10 mL) was added, and the vial was sealed and heated to 100 °C for 16 hours. After cooling to room temperature, the white precipitate that had formed was collected via filtration and washed with

dichloromethane and methanol. The ligand was collected as a white powder (1.011 g, 0.540 mmol, 87%). ¹H NMR (400 MHz, D₂O) δ 9.93 (s, 2H), 8.53 – 8.44 (m, 1H), 8.43 – 8.37 (m, 2H), 8.05 (dt, *J* = 8.2, 1.1 Hz, 2H), 7.88 (dt, *J* = 2.2, 1.3 Hz, 2H), 4.61 (t, *J* = 7.1 Hz, 4H), 3.11 – 3.03 (m, 4H), 2.50 (p, *J* = 7.2 Hz, 4H).

Scheme S1



Catalyst 1: Cat **1** was synthesized via the metalation shown in Scheme S1.² Ligand **1** (127 mg, 0.28 mmol) was dissolved in a mixture of 16 mL MeOH, 3 mL H₂O and Ag₂O (63 mg, 0.27 mmol) was added while excluding light. The suspension was stirred for 60 min at 50 °C, then NaCl (16 mg, 0.27 mmol) was added and the resulting suspension stirred vigorously for 15 min. The reaction mixture was then filtered and transferred to a solution of [Ru(*p*-cymene)Cl₂]₂ (98 mg, 0.16 mmol) in 10 mL H₂O. After stirring for 1 hour at room temperature the suspension was filtered and the solvent was removed *in vacuo*. The resulting residue was then extracted with MeOH (3 x 10 mL) and filtered. The orange solution was then reduced to 5 mL and precipitated with diethyl ether to form an orange solid. The solvent was decanted and the residue washed with Et₂O (3x10 mL) and dried *in vacuo* to yield complex **4** as an orange powder (46 mg, 0.063 mmol; 30%). ¹H NMR (d⁶-DMSO, 400 MHz): δ = 8.43 (d, J = 0.9 Hz, 1H), 8.35 (t, J = 1.0 Hz, 1H), 8.18 (d, J = 0.8 Hz, 1H), 8.15 (dd, J = 8.5, 1.0 Hz, 1H), 8.05 (d, J = 0.8 Hz, 1H), 7.75 (dd, J = 2.4, 0.8 Hz, 1H), 7.72 (d, J = 6.1 Hz, 1H), 6.12 (brs, 1H), 5.54 (d, J = 6.1 Hz, 1H), 5.43 (d, J = 6.1 Hz, 1H), 4.75 (brs, 1H), 4.62-4.32 (m, 4H), 2.90-2.68 (m 4H), 2.41-2.18 (m, 4H), 2.10-2.00 (m, 1H), 1.97 (s, 3H), 0.65 ppm (d, J = 6.8 Hz, 6H). ¹³C-NMR (DMSO, 100 MHz): δ=184.6, 153.9, 150.7, 146.3, 126.6, 126.2, 124.8, 123.0, 119.9, 116.2, 88.1, 50.0, 49.3, 48.1/47.5, 30.6, 25.7/25.1, 22.0/21.6, 18.6 ppm.

Reaction Procedure

All reactions were carried out in a high temperature-pressure autoclave (Parr®, 4564 series) fitted with a glass insert, standard mechanical agitator, and liquid sampling tube. The glass insert was loaded with catalyst, 25 mL of aqueous KOH (of desired concentration) and 25 mL of glycerol. The glass insert was then placed into the autoclave. The autoclave was sealed, and the stirrer turned on and set to 75% power. The autoclave was purged 5 times with CO₂ (Praxair, industrial grade) and pressurized to 10 bar. When the reaction reached the desired temperature, the pressure was adjusted to the desired operating conditions, typically 26 or 46 Bar. Reactions with carbonate were carried out in a similar manner, but pressurized with nitrogen instead of CO₂.

Product Characterization

Reaction aliquots were analyzed by HPLC and NMR. HPLC was performed using a Shimadzu Prominence-i (LC-2030C 3D) instrument equipped with a PDA detector using a mobile phase of 0.005 M H₂SO₄ with a flow rate of 0.44 mL/min at 35 °C. Samples for quantification of LA, FA and 1,2- PDO were prepared by adding a 1-mL aliquot of sample to 0.22 mL of 5 M H₂SO₄ and filtering with a syringe filter. The PDA detector scanned the range of 190-800 nm, affording traces at 190, 218, 254, and 284 nm for analysis. The 190-nm wavelength trace included glycerol and all the desired products, while the 218-nm trace excluded glycerol and 1,2-PDO. Typical HPLC trace and PDA chromatograms are shown in Figure S1. The retention times for LA, glycerol, FA and 1,2 PDO are 28.7, 29.5, 30.5, and 36 min respectively.

NMR was used to confirm HPLC yields and identity of products. For NMR analysis, a 0.100-mL aliquot of reaction solution was mixed with equal volume of standard solution of 3-(trimethylsilyl)propionic-2,2,3,3-d₄ acid sodium salt (TSP) and 0.5 mL D₂O. The only products identified by NMR were glycerol, LA, FA, 1,2-PDO and pyruvaldehyde (in minute amounts). Glycerol conversions were estimated to be < 5% in all reactions, but due to high glycerol concentrations used conversions could

not be accurately calculated from NMR or HPLC. A comparison was made with reactions in which the TSP standard was added at the beginning of reaction, rather than to each aliquot, and no major differences were observed.

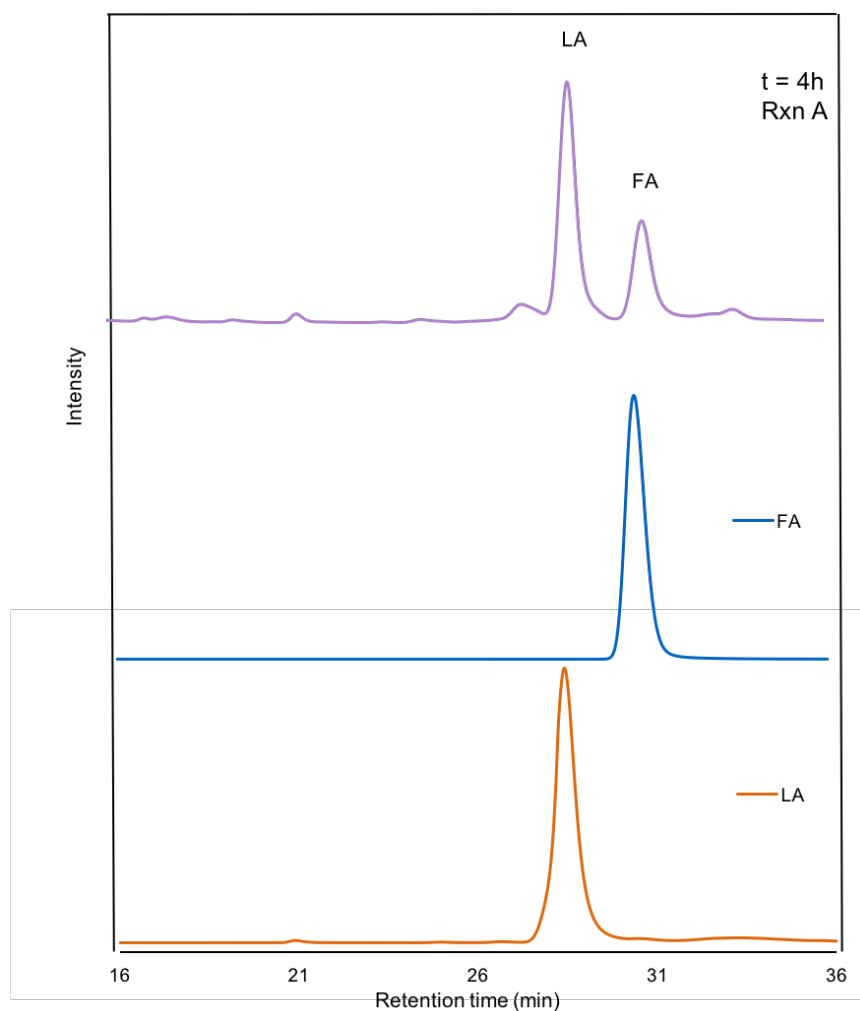


Figure S1: Extract from HPLC chromatogram traces at 218 nm wavelength, showing authentic formic acid (FA), lactic acid (LA) and the $t=4$ hr sample from Rxn A (6.85 M glycerol, catalyst *I* (5 mg), 150 °C, 26 bar CO₂, 2M KOH).

Calculation of free energies of reaction (ΔG_{aq})

All calculations were carried out using the G3B3 (or G3//B3LYP) method. This method is a variant of G3 theory, in which geometries are determined using the B3LYP/6-31G(d) method; energies are calculated at the MP4/6-31(d) level and corrected to QCISD(T)(full)/G3Large level using several additivity approximations at MP2 and MP4 levels. Geometries were fully optimized; all minima were verified to have no imaginary vibrational frequencies. Free energies were evaluated at 298 K. To estimate solvent effects, the self-consistent reaction-field (SCRF) continuum approach was employed using the IEF version of the polarizable continuum model (PCM) with parameters for water in single-point calculations on gas-phase geometries. All calculations were performed with the GAUSSIAN 16 software package.³

Table S1. Effect of temperature, pressure and KOH concentration on CO₂ transfer hydrogenation reactions from glycerol with cat *I*.

Entry	Temp (°C)	Pressure (bar)	[KOH] (M)	TON in 1 h		TON in 24 h		Final conc. (mM)	
				LA	FA	LA	FA	LA	FA
1	150	46	0.25	141	71	312	110	51.8	18.0
2	225	46	0.25	352	82	3297	280	328	27.9
3	150	46	1	28	28	360	330	56.2	49.8
4	150	46	2	58	57	356	329	59.4	55.1
5	150	46	0	0	0	0	0	0	0
6	225	46	0	88	26	206	141	60.4	48.6
7	150	26	2	38	38	632	586	95.5	86.3
8	180	26	2	520	348	1685	1065	262	166

Conditions: 6.85 M glycerol (1:1 water:glycerol), catalyst **1** (5 mg), 50 mL total volume, Parr autoclave. LA: Lactic Acid, FA: Formic Acid.

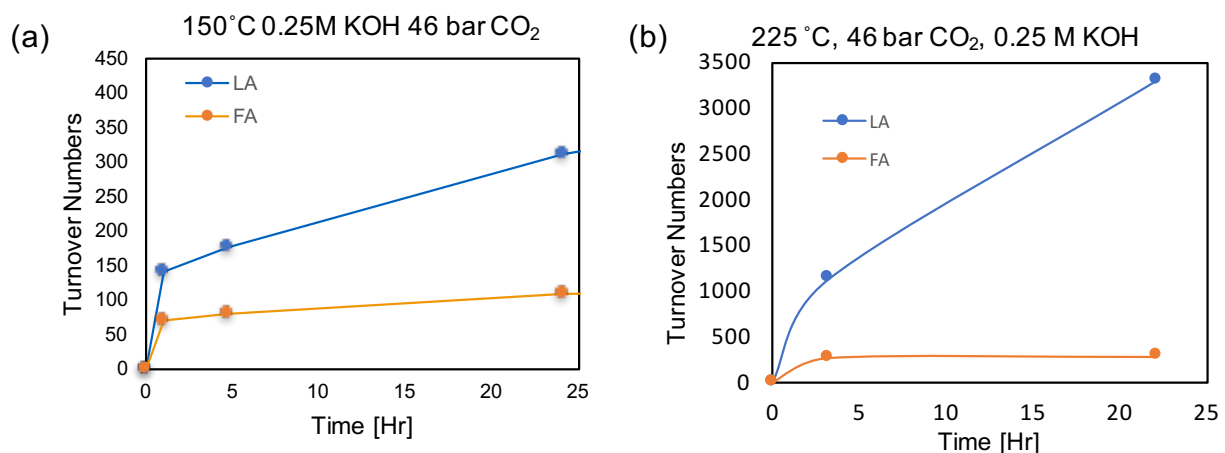


Figure S2. Time courses for production of formic acid (FA) and lactic acid (LA) from the reaction of CO₂ and glycerol using 46 bar CO₂, 6.85 M glycerol, and 0.25 M KOH at (a) 150 °C and (b) 225 °C.

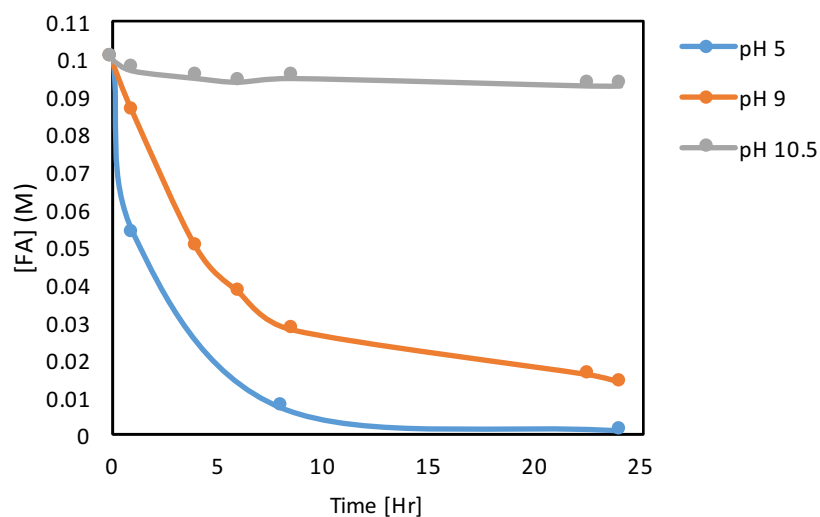


Figure S3. Time course for decomposition of formate in aqueous medium using catalyst *I* at 150 °C (0.15 mM cat *I*, 0.10 M formic acid, KOH(aq) to adjust pH, 50 mL total volume of water).

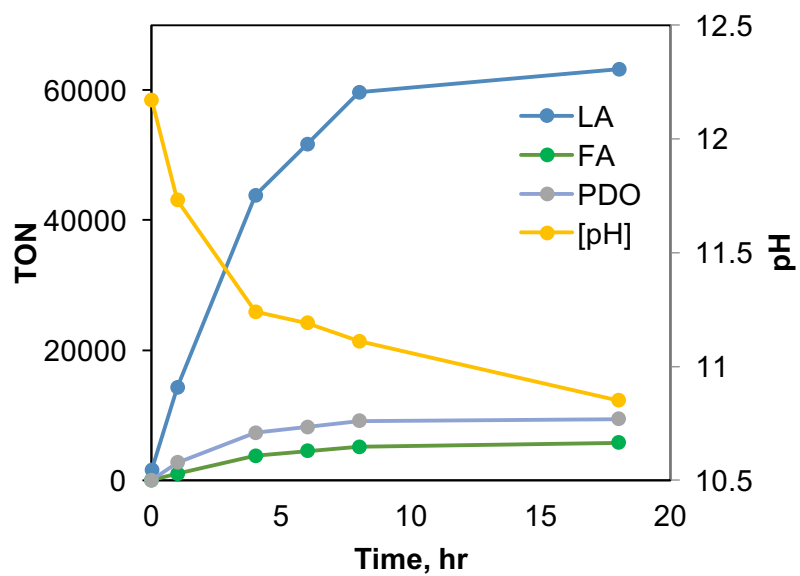


Figure S4. Additional visualization of the time course of reaction of K_2CO_3 and glycerol using catalyst *1* (pN_2 26 Bar, 6.85 M aqueous glycerol, 2.00 M K_2CO_3 , at 150 °C).

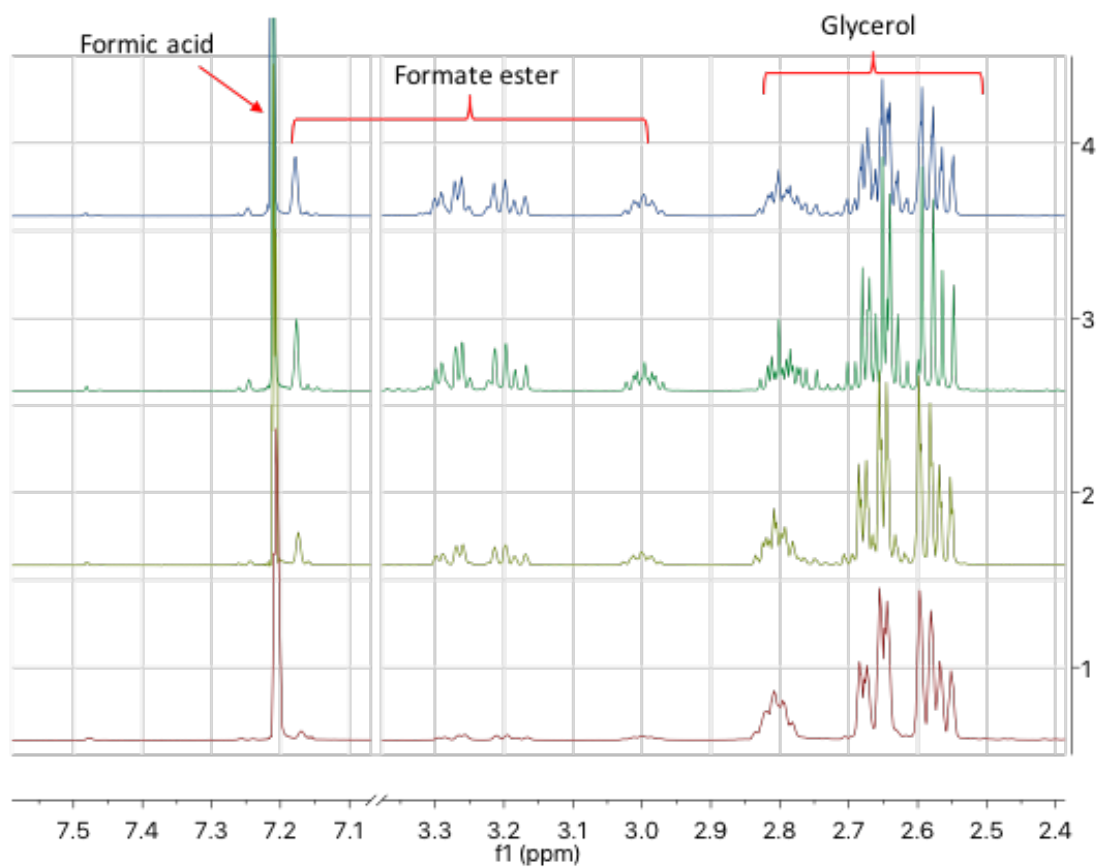


Figure S5. Section of ¹H NMR spectra corresponding to t=0 (1), t=30 min (2), t=1h; t=90 min (3), for reaction of formic acid and glycerol to afford formate ester.

Table S2. Calculated free energies of reaction (ΔG_{aq}°) for the CO₂ direct hydrogenation and transfer hydrogenation (Gaussian16, G3B3, PCM water).

Entry		ΔG_{aq}° (kcal/mol)
1a	$\text{CO}_2 + \text{H}_2 \longrightarrow \text{H}-\overset{\text{O}}{\parallel}{\text{C}}-\text{OH}$	13.4
1b	$\text{CO}_2 + \text{H}_2 + \text{OH}^- \longrightarrow \text{H}-\overset{\text{O}}{\parallel}{\text{C}}-\text{O}^- + \text{H}_2\text{O}$	-40.6
2a	$\text{CO}_2 + \text{CH}_3\text{CH}(\text{OH})\text{CH}_3 \longrightarrow \text{H}-\overset{\text{O}}{\parallel}{\text{C}}-\text{OH} + \text{CH}_3\text{C}(=\text{O})\text{CH}_3$	3.70
2b	$\text{CO}_2 + \text{CH}_3\text{CH}(\text{OH})\text{CH}_3 \longrightarrow \text{H}-\overset{\text{O}}{\parallel}{\text{C}}-\text{O}^- + \text{CH}_3\text{C}(=\text{O})\text{CH}_3 + \text{H}_2\text{O}$	-50.3
3	$\text{CO}_2 + \text{HOCH}_2\text{CH}(\text{OH})\text{CH}_2\text{OH} \longrightarrow \text{H}-\overset{\text{O}}{\parallel}{\text{C}}-\text{OH} + \text{HOCH}_2\text{C}(=\text{O})\text{CH}_2\text{OH}$	12.3
3b	$\text{CO}_2 + \text{HOCH}_2\text{CH}(\text{OH})\text{CH}_2\text{OH} + \text{OH}^- \longrightarrow \text{H}-\overset{\text{O}}{\parallel}{\text{C}}-\text{O}^- + \text{HOCH}_2\text{C}(=\text{O})\text{CH}_2\text{OH} + \text{H}_2\text{O}$	-41.8
4a	$\text{CO}_2 + \text{HOCH}_2\text{CH}(\text{OH})\text{CH}_2\text{OH} \longrightarrow \text{H}-\overset{\text{O}}{\parallel}{\text{C}}-\text{OH} + \text{HOCH}_2\text{C}(=\text{O})\text{CH}_2\text{OH}$	-9.21
4b	$\text{CO}_2 + \text{HOCH}_2\text{CH}(\text{OH})\text{CH}_2\text{OH} + 2\text{OH}^- \longrightarrow \text{H}-\overset{\text{O}}{\parallel}{\text{C}}-\text{O}^- + \text{HOCH}_2\text{C}(=\text{O})\text{CH}_2\text{O}^- + 2\text{H}_2\text{O}$	-119
5	$\text{HCO}_3^- + \text{H}_2 \longrightarrow \text{H}-\overset{\text{O}}{\parallel}{\text{C}}-\text{O}^- + \text{H}_2\text{O}$	4.44
6	$\text{HCO}_3^- + \text{HOCH}_2\text{CH}(\text{OH})\text{CH}_2\text{OH} \longrightarrow \text{H}-\overset{\text{O}}{\parallel}{\text{C}}-\text{O}^- + \text{HOCH}_2\text{C}(=\text{O})\text{CH}_2\text{OH} + \text{H}_2\text{O}$	-83.9

References

1. Godoy, F.; Segarra, C.; Poyatos, M.; Peris, E., *Organometallics* **2011**, *30* (4), 684-688.
2. Jantke, D.; Cokoja, M.; Pöthig, A.; Herrmann, W. A.; Kühn, F. E., *Organometallics* **2013**, *32* (3), 741-744.
3. Frisch, M. J.; Trucks, G. W.; Schlegel, H. B.; Scuseria, G. E.; Robb, M. A.; Cheeseman, J. R.; Scalmani, G.; Barone, V.; Mennucci, B.; Petersson, G. A.; Nakatsuji, H.; Caricato, M.; Li, X.; Hratchian, H. P.; Izmaylov, A. F.; Bloino, J.; Zheng, G.; Sonnenberg, J. L.; Hada, M.; Ehara, M.; Toyota, K.; Fukuda, R.; Hasegawa, J.; Ishida, M.; Nakajima, T.; Honda, Y.; Kitao, O.; Nakai, H.; Vreven, T.; Montgomery, J. A.; Peralta, J. E.; Ogliaro, F.; Bearpark, M.; Heyd, J. J.; Brothers, E.; Kudin, K. N.; Staroverov, V. N.; Kobayashi, R.; Normand, J.; Raghavachari, K.; Rendell, A.; Burant, J. C.; Iyengar, S. S.; Tomasi, J.; Cossi, M.; Rega, N.; Millam, J. M.; Klene, M.; Knox, J. E.; Cross, J. B.; Bakken, V.; Adamo, C.; Jaramillo, J.; Gomperts, R.; Stratmann, R. E.; Yazyev, O.; Austin, A. J.; Cammi, R.; Pomelli, C.; Ochterski, J. W.; Martin, R. L.; Morokuma, K.; Zakrzewski, V. G.; Voth, G. A.; Salvador, P.; Dannenberg, J. J.; Dapprich, S.; Daniels, A. D.; Farkas; Foresman, J. B.; Ortiz, J. V.; Cioslowski, J.; Fox, D. J., Gaussian 09, Revision B.01. Wallingford CT, 2009.